Hydration Dynamics of Hyaluronan and Dextran

Johannes Hunger,*,‡ Anja Bernecker,† Huib J. Bakker,* Mischa Bonn,*,‡ Ralf P. Richter†,§

*Fundamenteel Onderzoek der Materie (FOM) Institute AMOLF, Amsterdam, The Netherlands
‡Max Planck Institute for Polymer Research, Mainz, Germany
†Center for Cooperative Research in Biosciences (CIC biomaGUNE), San Sebastián, Spain
§Max Planck Institute for Intelligent Systems, Stuttgart, Germany

Supporting Material

Materials

Hyaluronic acid sodium salt (hyaluronan, HA) from rooster comb (molecular weight 1 to $4 \cdot 10^6\,\mathrm{g\,mol^{-1}}$) and dextran from *Leuconostoc mesenteroides* (analytic standard grade, molecular weight $1.4 \cdot 10^6\,\mathrm{g\,mol^{-1}}$, $\sim 5\,\%$ branched) were purchased from Sigma Aldrich and used without further purification. Samples with different weight fractions, w, (g of polysaccharide / g of solution) were prepared using an analytical balance. Dextran was dissolved in ultrapure water at the desired concentrations and shaken for 2 h at room temperature. HA was dissolved in ultrapure water and shaken overnight at 40 °C. The hyaluronic acid salt samples were centrifuged several times for 10 min at 10000 rpm to obtain a homogeneous solution. For femtosecond-infrared experiments a small amount ($\sim 4\,\%$ (w/w)) deuterium oxide (99.97 %D from Euriso-top, Saint-Aubin, France) was added to the ultrapure water before dissolving dextran or HA. Due to fast isotopic exchange, we obtain the equilibrium distribution of deuterium atoms among all acidic protons. Therefore the dominant isotopically labeled species are HOD molecules.

For analysis of the Terahertz (THz) experiments, molar concentrations (in $\mathrm{mol\,L^{-1}}$) of water, $c_{\mathrm{H_2O}}$, in the sample are required. These were calculated from the weight fractions, w, using solution densities, ρ, interpolated from literature ($\rho(\mathrm{dextran}) = (997.05 + 410 \cdot w)\,\mathrm{g\,L^{-1}}$; $\rho(\mathrm{HA}) = (997.05 + 440 \cdot w)\,\mathrm{g\,L^{-1}}$) [1, 2, 3].

Polarization-resolved femtosecond-infrared spectroscopy

Experimental method

Femtosecond infrared pump and probe pulses were generated via a sequence of nonlinear optical conversion processes that are pumped by a commercial Ti:sapphire regenerative amplified laser system (Spectra-Physics Hurricane, USA). This system delivers pulses at 800 nm with a duration of 100 fs at a repetition rate of 1 kHz (1 mJ per pulse). Approximately 0.7 mJ of pulse energy is used to pump an optical parametric amplifier based on a β-barium borate crystal. The optical parametric amplifier is used to generate idler pulses at $\sim 2\,\mu$m, which are subsequently frequency-doubled in a second β-barium borate crystal, yielding pulses at $\sim 1\,\mu$m. In a second parametric amplification process in a lithium niobate crystal the 1 μm pulses are used as a seed and the remaining 800 nm pulses (0.3 mJ) as a pump to generate mid-infrared pulses with a duration of ~ 150 fs and an energy of $\sim 6\,\mu$J. The frequency of these pulses is centered at $2500\,\mathrm{cm^{-1}}$, which coincides with the absorption of the O-D stretching vibration of HOD molecules (Note that the N-D stretch vibration, which is formed via isotopic exchange with HOD absorbs at similar wavenumbers. Its contribution to our experiments, however, is negligible [4]).

A CaF_2 wedged window is used to split the mid-infrared pulses into a pump ($\sim 92\,\%$), a probe ($\sim 4\,\%$), and a reference ($\sim 4\,\%$) pulse. The polarization of the pump pulse is rotated by 45 ° with respect to the probe and the reference polarization using a $\lambda/2$ plate. The time delay of the probe pulses with respect to the pump is varied via a variable path-length delay line. The pump pulse is modulated using

an optical chopper. The three pulses are focused into the sample with an off-axis parabolic mirror. In the sample, which is held between two CaF_2 windows, the foci of the probe and pump-pulse overlap. After passing a polarizer that allows us to select the parallel or perpendicular (with respect to the pump) polarization components, the probe and reference beams are sent into a spectrometer dispersing the beams on a liquid-nitrogen-cooled mercury-cadmium telluride detector. The probe pulse is used to measure the (pump-induced) transient absorption in the sample parallel ($\Delta\alpha_{\parallel}(\omega, t)$) and perpendicular ($\Delta\alpha_{\perp}(\omega, t)$) to the pump polarization as a function of delay time, t, and wavenumber, ω. The reference pulse is used for a spectrally resolved correction of the pulse to pulse energy fluctuations [5].

Data Analysis

From the measured absorption changes $\Delta\alpha_{\parallel}(\omega, t)$ and $\Delta\alpha_{\perp}(\omega, t)$ we construct the isotropic signal:

$$\Delta\alpha_{\mathrm{iso}}(\omega, t) = \frac{\Delta\alpha_{\parallel}(\omega, t) + 2\Delta\alpha_{\perp}(\omega, t)}{3} \tag{S1}$$

The isotropic signal is independent of reorientation processes and is dominated by the vibrational relaxation of the excitation and by the dynamics of any consecutive processes. At short delays the isotropic signal is dominated by the vibrational excitation of the OD oscillators. The vibrational energy relaxes to an intermediate state (i.e. intermediate energy levels) and eventually leads to heating of the sample by a few degrees (low energy levels) [6, 7, 8]. At long delay times ($t > 20\,\mathrm{ps}$) this heating effect prevails. To obtain the anisotropy dynamics, $R(t)$ of the excited OD-stretch transition dipoles, we correct the measured signals $\Delta\alpha_{\parallel}(\omega, t)$ and $\Delta\alpha_{\perp}(\omega, t)$ for this time-dependent thermalization of the sample. The evolution of the thermalization is obtained via detailed analysis of $\Delta\alpha_{\mathrm{iso}}(\omega, t)$ following the route described in detail in Ref. [10]. To briefly summarize, we fit a kinetic model to the isotropic data. In this model the pump pulse generates a population in the first vibrational excited state. This excitation transiently populates an intermediate state with a characteristic time constant of $\sim 1.7\,\mathrm{ps}$. For the present samples this time is virtually constant at all concentrations of polysaccharide. The intermediate state has the same absorption spectrum as the vibrational ground state (i.e. the transient absorption equals zero). The intermediate state further relaxes to the final thermal state with a characteristic time constant of $\sim 1\,\mathrm{ps}$ for solutions of 8 % HOD in H_2O. For the present samples this equilibration time is increasing smoothly as the concentration of polysaccharide increases. At the highest concentration (20 % (w/w)) of polysaccharide the equilibration occurs on a $\sim 1.5\,\mathrm{ps}$ timescale. This slow-down of the equilibration indicates a slower equilibration of the samples to the thermal disturbance and/or the appearance of additional intermediate energy levels.

From this analysis, the spectral signature and the temporal evolution of the thermalization is obtained, which is subsequently subtracted from the raw transient spectra ($\Delta\alpha_{\parallel}(\omega, t)$ and $\Delta\alpha_{\perp}(\omega, t)$). The thus obtained corrected transient spectra, $\Delta\alpha'_{\parallel}(\omega, t)$ and $\Delta\alpha'_{\perp}(\omega, t)$ solely reflect the signal originating from the excited OD oscillators.

From the corrected signals we construct the anisotropy parameter $R(t)$:

$$R(\omega, t) = \frac{\Delta\alpha'_{\parallel}(\omega, t) - \Delta\alpha'_{\perp}(\omega, t)}{\Delta\alpha'_{\parallel}(\omega, t) + 2\Delta\alpha'_{\perp}(\omega, t)}. \tag{S2}$$

$R(t)$ directly corresponds to the second order rotational correlation time of the excited OD oscillators [9]. $R(t)$ decays are averaged over frequencies ranging from $2460\,\mathrm{cm}^{-1}$ to $2540\,\mathrm{cm}^{-1}$ as it is independent of absorption frequency [10].

The thus obtained anisotropies are inconsistent with all water molecules having the same rotational dynamics (as for neat water [7]), which is described by a single exponential decay of $R(t)$ (see Figure S1). Hence, we model the experimental anisotropies with a double exponential decay (eq 1), which excellently describes the observed rotational dynamics of the HOD molecules (see Figures 1 & S1). From these fits we obtain a rotational correlation time of $\tau_{\mathrm{s,IR}} \gg 10\,\mathrm{ps}$ at all concentrations, if all parameters of eq 1 are allowed to vary. This means that the rotational dynamics of the slow subensemble of water molecules are essentially static on the 5 ps time-scale of our experiment. To reduce the number of free parameters, we fix the rotation times of the slowed down subensemble of water to $\tau_{\mathrm{s,IR}} \approx \infty$ ($t/\tau_{\mathrm{s,IR}} \approx 0$).

Terahertz time-domain spectroscopy

Experimental method

Terahertz pulses are generated in a ZnTe (110) nonlinear crystal [11] from 800 nm pulses with a duration of $\sim$ 150 fs from a Ti:Sapphire laser (Coherent Legend Elite, USA). The generated THz pulses have a duration of $\sim$ 1 ps. The time-dependent electric field of the THz pulse is measured via its electro-optic effect on a variably delayed 800 nm laser pulse in a second ZnTe crystal. A frequency domain analysis of the THz pulse transmitted through an empty cell and the THz pulse transmitted through a filled sample cell yields the frequency dependent complex index of refraction ($\hat{n}(\nu) = n(\nu) - \mathrm{i}k(\nu)$) as function of field frequency, ν (ranging from 0.4 to 1.2 THz). In analysing the data, all (multiple) reflection and transmission coefficients for all transitions (air-window-sample-window-air) were taken into account [12]. To minimize the effect of fluctuations in the THz intensity, a rotating sample cell with two separate sample compartments is used to position the sample and a pure water reference alternatingly in the focus of the THz beam. The sample is held between two Polychlorotrifluoroethylene windows separated by a teflon spacer (thickness $\sim 100\,\mu$m). The neat water data were used to calibrate the spectra of the samples.

Data Analysis

Complex refractive index spectra were converted to complex permittivity spectra, $\hat{\varepsilon}(\nu)$ ($= \hat{n}^2(\nu)$). For neat water $\hat{\varepsilon}(\nu)$ is dominated by an intense relaxation mode at $\sim$ 20 GHz that can be well described with a Debye equation (i.e. a single exponential decay of the orientational polarization of the sample in the time-domain) [13]. This relaxation originates from the partial alignment of the (dipolar) water molecules to the external electric field. For neat water a characteristic collective first-order orientational relaxation time of $\tau_1 = 8.3$ ps is observed at ambient temperature [13]. Its amplitude is found to be $S_1 = 72$. Further, a weak Debye-type high-frequency mode centered at ~ 0.5 THz is observed with an amplitude $S_2 \approx 1.3$ and relaxation time $\tau_2 \approx 200$ fs. Thus, we model the experimental spectra with a superposition of two Debye-type relaxation modes:

$$\hat{\varepsilon}(\nu) = \frac{S_1}{1 + 2\pi\nu\mathrm{i}\tau_1} + \frac{S_2}{1 + 2\pi\nu\mathrm{i}\tau_2} + \varepsilon_\infty \tag{S3}$$

where ε_∞ represents the high-frequency limit of the permittivity. ε_∞ subsumes all electronic and intramolecular polarizations at infrared and optical frequencies. Following previous work [14], τ_1 was fixed to the value obtained from the reference sample (pure water) using the known static permittivity of water, $\varepsilon = S_1 + S_2 + \varepsilon_\infty = 78.368$ [15]. τ_2, S_1, S_2, and ε_∞ are the independent fit parameters. The thus obtained amplitude S_1 can be converted to the molar concentration of unaffected (bulk-like) water molecules, c_b using the Cavell equation [16, 17]:

$$c_\mathrm{b} = \frac{k_\mathrm{B} T \varepsilon_0}{N_\mathrm{A}} \frac{2\varepsilon + 1}{\varepsilon} \cdot S_1 \cdot \frac{1}{\mu_\mathrm{eff}^2} \tag{S4}$$

where N_A and k_B are the Avogadro and Boltzmann constant, respectively and T is the thermodynamic temperature. μ_eff is the effective dipole moment of water in solution. μ_eff was assumed to be constant and the same as for neat water $\mu_\mathrm{eff} = 3.8\,\mathrm{D}$ ($1\,\mathrm{D} = 3.33564 \times 10^{-30}\,\mathrm{Cm}$) [13, 18].

Supporting Figure

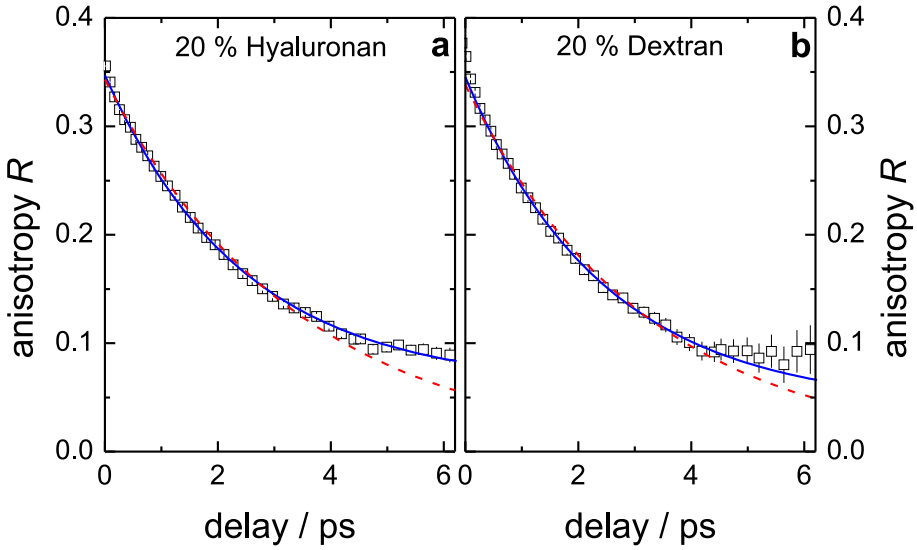

Figure S1: Anisotropy parameter, $R(t)$, for the OD stretch vibration for solutions of 20 % hyaluronan (a) and 20 % dextran (b) in isotopically diluted water (8 % HOD in H_2O). Dashed red lines correspond to fits of a single exponential decay to the experimental data. Solid blue lines show the fits with a double exponential decay (eq 1).

References

[1] Gómez-Alejandre, S., E. Sánchez de la Blanca, C. Abradelo de Usera, M. F. Rey-Stolle, and I. Hernández-Fuentes. 2000. Partial specific volume of hyaluronic acid in different media and conditions. *Int. J. Biol. Macromol.* 27:287–290.

[2] Kany, H.-P., H. Hasse, and G. Maurer. 1999. Thermodynamic properties of aqueous dextran solutions from laser-light-scattering, membrane osmometry, and isopiestic measurements. *J. Chem. Eng. Data*. 44:230–242.

[3] Akashi, N., J.-I. Kushibiki, and F. Dunn. 2000. Measurements of acoustic properties of aqueous dextran solutions in the VHF/UHF range. *Ultrasonics*. 38:915–919.

[4] Rezus, Y. L. A., and H. J. Bakker. 2006. Effect of urea on the structural dynamics of water. *Proc. Natl. Acad. Sci. U.S.A.* 103:18417–18420.

[5] Bakker, H. J., Y. L. A. Rezus, and R. L. A. Timmer. 2008. Molecular reorientation of liquid water studied with femtosecond mid-infrared spectroscopy. *J. Phys. Chem. A*. 112:11523–11534.

[6] Steinel, T., J. B. Asbury, J. Zheng, and M. D. Fayer. 2004. Watching hydrogen bonds break: A transient absorption study of water. *J. Phys. Chem. A*. 108:10957–10964.

[7] Rezus, Y. L. A., and H. J. Bakker. 2006. Orientational dynamics of isotopically diluted H_2O and D_2O. *J. Chem. Phys.* 125:144512.

[8] Bakker, H. J., and J. L. Skinner. 2010. Vibrational spectroscopy as a probe of structure and dynamics in liquid water. *Chem. Rev.* 110:1498–1517.

[9] Graener, H., Seifert, G. and A. Laubereau. 1990. Direct observation of rotational relaxation times by time-resolved infrared spectroscopy. *Chem. Phys. Lett.* 172:435–439.

[10] Rezus, Y. L., and H. J. Bakker. 2005. On the orientational relaxation of HDO in liquid water. *J. Chem. Phys.* 123:114502.

[11] Ahn, J., A. V. Efimov, R. D. Averitt, and A. J. Taylor. 2003. Terahertz waveform synthesis via optical rectification of shaped ultrafast laser pulses. *Opt. Express*. 11:2486–2496.

[12] Knoesel, E., M. Bonn, J. Shan, F. Wang, and T. F. Heinz. 2004. Conductivity of solvated electrons in hexane investigated with terahertz time-domain spectroscopy. *J. Chem. Phys.* 121:394-404.

[13] Fukasawa, T., T. Sato, J. Watanabe, Y. Hama, W. Kunz, and R. Buchner. 2005. Relation between dielectric and low-frequency Raman spectra of hydrogen-bond liquids. *Phys. Rev. Lett.* 95:197802.

[14] Tielrooij, K. J., R. L. A. Timmer, H. J. Bakker, and M. Bonn. 2009. Structure dynamics of the proton in liquid water probed with terahertz time-domain spectroscopy. *Phys. Rev. Lett.* 102:198303.

[15] Fernández, D. P., A. R. H. Goodwin, E. W. Lemmon, J. M. H. Levelt Sengers, and R. C. Williams. 1997. A formulation of the static permittivity of water and steam at temperatures from 283 K to 873 K at pressures up to 1200 MPa, including derivatives and Debye–Hückel coefficients. *J. Phys. Chem. Ref. Data*. 26:1125–1166.

[16] Cavell, E. A. S., P. C. Knight, and M. A. Sheikh. 1971. Dielectric relaxation in non aqueous solutions. part 2. Solutions of tri(n-butyl)ammonium picrate and iodide in polar solvents. *Trans. Faraday Soc.* 67:2225–2233.

[17] Hunger, J., A. Stoppa, R. Buchner, and G. Hefter. 2009. Dipole correlations in the ionic liquid 1-N-ethyl-3-N-methylimidazolium ethylsulfate and its binary mixtures with dichloromethane. *J. Phys. Chem. B*. 113:9527– 9537.

[18] Hunger, J., K. J. Tielrooij, R. Buchner, M. Bonn, and H. J. Bakker. 2012. Complex formation in aqueous trimethylamine-N-oxide (TMAO) solutions. *J. Phys. Chem. B*. 116:4783–4795.